A New Dimension in Retrograde Flow: Centripetal Movement of Engulfed Particles

Avi Caspi,* Orna Yeger,† Inna Grosheva,‡ Alexander D. Bershadsky,‡ and Michael Elbaum*
*Department of Materials and Interfaces, †Electron Microscopy Unit, and ‡Department of Molecular Cell Biology, Weizmann Institute of Science, Rehovot 76100, Israel

ABSTRACT Centripetal motion of surface-adherent particles is a classic experimental system for studying surface dynamics on a eukaryotic cell. To investigate bead migration over the entire cell surface, we have developed an experimental assay using multinuclear giant fibroblasts, which provide expanded length scales and an unambiguous frame of reference. Beads coated by adhesion ligands concanavalin A or fibronectin are placed in specific locations on the cell using optical tweezers, and their subsequent motion is tracked over time. The adhesion, as well as velocity and directionality of their movement, expose distinct regions of the cytoplasm and membrane. Beads placed on the peripheral lamella initiate centripetal motion, whereas beads placed on the central part of the cell attach to a stationary cortex and do not move. Careful examination by complementary three-dimensional methods shows that the motion of a bead placed on the cell periphery takes place after engulfment into the cytoplasm, whereas stationary beads, placed near the cell center, are not engulfed. These results demonstrate that centripetal motion of adhering particles may occur inside as well as outside the cell. Inhibition of actomyosin activity is used to explore requirements for engulfment and aspects of the bead movement. Centripetal movement of adherent particles seems to depend on mechanisms distinct from those driving overall cell contractility.

INTRODUCTION

Centripetal motion of surface-adherent particles is a classic experimental system (Abercrombie et al., 1970; Harris and Dunn, 1972) for the study of surface dynamics on living cells. On the leading edge of substrate-adherent, motile cells, a micron-sized particle will move centripetally, i.e., from the cell edge toward the nuclear region. Experiments based on centripetal movement of attached microspheres have been performed on many types of eukaryotic cells, including *Dictyostellium amoeba* (Jay and Elson, 1992), fish keratocytes (Anderson et al., 1996; Galbraith and Sheetz, 1999), fibroblasts (Schmidt et al, 1993; Choquet et al., 1997), and neuronal growth cones (Lin and Forscher, 1995). Such experiments are motivated by the assumption that the rearward motion of particles attached to the dorsal cell surface reflects a mechanism which, on the ventral side, would have acted on the substrate to provide traction forces drawing the cell forward. Several models have been proposed to explain centripetal motion of surface-bound particles. These may be grouped broadly into those based on lipid membrane flow (Bretscher, 1984), and those based on a transmembrane interaction with a submembranous cortex of moving or polymerizing actin (Sheetz et al., 1989; Lin and Forscher, 1995; Lin et al., 1996). The latter are normally associated with specific ligand recognition (Choquet et al., 1997; Felsenfeld et al., 1999). Both paradigms are based on the classical observations that adherent particles execute their motion entirely outside the cell and thereby act as surface markers.

Results presented here show that, at least in a particular cellular model, surface-adherent beads may perform their canonical centripetal motion after engulfment into the cytoplasm, beneath the plane of the free dorsal membrane. Thus, adherent beads do not necessarily reflect the motion of surface-associated structures. This is substantiated by scanning electron microscopy (SEM) following optical observation, as well as by live observation with three-dimensional particle tracking. We find that the membrane is divided radially into two distinct regions with respect to adhesion, and the cytoplasm into three regions with respect to particle motion over the path of the bead from the cell edge to the perinuclear area. Beads that adhere near the edge, on the lamella, are engulfed and move. Adhesion to the central regions of the cell is selective, dependent on the bead coating. We suggest that the retrograde flow of intracellular filamentous actin (F-actin) (Waterman-Storer et al., 1998; Henson et al., 1999), in contrast to flow of lipid or movement of a submembranous cortex, is responsible for our observations of centripetal particle movement.

MATERIALS AND METHODS

Cells

The SV80 line of immortalized human fibroblasts (Todaro et al., 1966) was used for all experiments. Cells were cultured in Dulbecco's modified Eagle medium (DMEM) containing 10% bovine calf serum at 37°C and 7.5% CO_2 and passaged by versene-trypsin solution. Multinuclear giants were produced from sparse cultures by addition of cytochalasin D to the medium at 0.2 μg/ml concentration for 3 to 5 days. Cells were washed with fresh medium and left for ~1 h before replating into observation chambers, again in serum-containing DMEM.

Received for publication 27 July 2000 and in final form 9 July 2001.

Address reprint requests to Dr. Michael Elbaum, Dept of Materials and Interfaces, Weizmann Institute of Science, Rehovot 76100, Israel. Tel.: 972-8-9343537; Fax: 972-8-9344138; E-mail: michael.elbaum@weizmann.ac.il.

0006-3495/01/10/1990/11 $2.00

Bead Preparation

Protein coatings were made at saturating concentrations on 3-μm diameter polystyrene latex beads with amine surface functionalization (Polysciences, Inc., Warrington, PA) following the manufacturer's protocol for glutaraldehyde activation. Concanavalin A (ConA, catalog no. C-7275) and human fibronectin (FN, catalog no. F-2006) were obtained from Sigma Israel Chemical Co. (Rehovot, Israel). For ConA, simple adsorption to the beads by incubation was also sufficient to induce all effects described here.

Live cell observation

Observation chambers were prepared from 35 mm petri dishes with 6 mm diameter holes cut in the bottoms. Eppendorf CellLocate coverslips (Eppendorf AG, Hamburg, Germany) with 55-μm spacing were fixed to the plastic dishes with Parafilm (American National Can Co., Menasha, WI). The glass-bottom dishes were pre-incubated in serum-containing medium for at least 5 h to promote cell adhesion.

Giant cells were passed onto observation chambers the day before use by trypsinization and very gentle centrifugation. Before observation the medium was exchanged for Leibowitz L-15 medium, either serum-free or containing 10% bovine calf serum. The pH buffering in this medium is not sensitive to CO_2. In case the culture cells were treated with a specific drug (see below), we also added the same drug to the L-15 medium. The dish was then covered by a lid with a round glass coverslip making contact with the fluid to prevent evaporation, and mounted on the microscope stage.

Observations were made on a differential interference contrast (DIC)-equipped inverted microscope (Axiovert 35, Carl Zeiss, Inc. Göttingen, Germany) with a Fluar 100 ×/1.3 NA oil-coupled objective followed by a 0.5X demagnification lens. DIC imaging was used for presentation purposes, whereas brightfield gave best accuracy for measurements on the large beads. The objective was maintained at 37°C by an electric heating band (Bioptechs Inc., Butler, PA). Thermal conductivity through the immersion oil held the cells at the same temperature. Individual SV80 cells under these conditions were motile and dividing, even reaching confluence on the microscope stage. Images were acquired by a ½″ digital charge coupled device video camera (iSight, Tirat haCarmel, Israel, model iSC2050LL) and recorded to S-VHS video cassettes.

Cytoskeletal inhibitors

Reagents were obtained from Sigma Israel Chemical Co. BDM (2, 3-butanedione monoxime, catalog no. B-0753) was used as a myosin inhibitor at 10 mM concentration by replacing half the L15 medium in the observation chamber with a medium containing the drug at double concentration. The kinase inhibitor H-7 (1-(5-isoquinolinesulfonyl)-2-methyl-piperazine dihydrochloride, catalog no. I-7016) was used at a concentration of 90 μM. It was added to the DMEM 5 h before observation, after which the medium was replaced by L-15 containing the drug at the same concentration. A similar procedure was applied for microtubule depolymerization by nocodazole (methyl-(5-[2-thienylcarbonyl][^{1}H]benzimidazol-2-yl) carbamate, catalog no. M-1404) at 10 μM overnight. Transfection by a plasmid encoding a chimera of the actomyosin regulatory protein caldesmon and green fluorescent protein (GFP) (Helfman et al., 1999) was performed directly on giant cells using calcium phosphate, a day before observation. Transfected cells were identified in the culture by their fluorescence.

Particle tracking

Particle-tracking analysis was performed offline using a cross-correlation algorithm that provides subpixel resolution (Gelles et al., 1988). The pixel size in our optical arrangement corresponds to 160 nm in the sample. Image sequences were captured by personal computer equipped with a Matrox Meteor frame grabber (Matrox, Inc., Dorval, Quebec, Canada). The Matrox Inspector software package contains a cross-correlation based algorithm for object localization, which was used for the bead tracking. Further analysis was made using Matlab and Excel.

Fixation and staining

Cells were fixed for phalloidin staining and for SEM while on the microscope stage, to arrest the observed state as quickly as possible and to permit a return to the same cells and beads in the later observations. Fixatives were used first at double the normal concentration, doubling the volume in the observation dish. They were replaced after 10 min with fresh fixative at normal concentration.

For fluorescent F-actin, cells were fixed in 3% paraformaldehyde for 20 min, followed by permeabilization with 0.5% Triton X-100 in phosphate-buffered saline for 2 min. Coverslips were broken away from the petri dish by gentle pressure. Cells were then incubated in rhodamine-phalloidin for 1 h, rinsed thoroughly with phosphate-buffered saline, and mounted on slides using elvanol. Fluorescence observations (not shown) were made by epifluorescence in the inverted microscope. Fig. 2 *d* was made using an Olympus Fluoview200 confocal laser scanning microscope with UPlanApo 60/1.4 objective.

For SEM, cells were fixed and prepared as reported (Levenberg et al., 1998). Coverslips were removed from the dishes before critical-point drying and examined by optical microscopy throughout the steps of preparation. Specimens were observed in a JEOL GMC 6400 SEM with accelerating voltage 20 kV.

Optical tweezers

Optical tweezers (Ashkin et al., 1986) were used to place the beads on the dorsal surface of the giant cells. The tweezers are based on a 200 mW infrared laser diode with output at 830 nm (SDL Inc., San Jose, CA, model SDL-5432-H1). The beam is directed through the epifluorescence port of the microscope and toward the objective using a dichroic mirror (Chroma Technology, Brattleboro, VT, part no. 750DCSP) mounted in the fluorescence-filter holder. The maximum escape force for a 3-μm bead was calibrated at 17 pN by scanning the stage horizontally and holding the bead against the resulting Stokes drag.

Height measurements

Measurement of the height of a bead relative to the plane of focus can be made by interpretation of the out of focus image. This is done most sensitively by illuminating in brightfield with collimated light (Strick et al. 1998). Diffraction rings then appear around beads that are not perfectly in focus, as shown in Fig. 4. The number and diameter of the rings provide a measure of the distance from the focal plane. A straightforward analysis is to match the image to a series of frames recorded at predetermined heights using the cross-correlation algorithm. Each frame represents a height relative to an arbitrary plane. The matching score of the correlation between the test and reference images is then plotted as a function of the frame number, and the best correlation determines the measured height. Performing the above procedure for two nearby beads gives the relative difference in height.

To measure the height of an engulfed bead relative to the dorsal membrane surface of the cell, we compared the test bead with a bead placed nearby on top of the cell using the optical tweezers. To trace the moving bead height dynamically, a reference bead was attached to the coverslip surface nearby the chosen cell. A frame-by-frame comparison was then made between the height of the moving bead and the reference. This procedure automatically corrects for slow drift in the microscope body and stage.

RESULTS

Experiments were performed on multinuclear giant cells, based on the SV80 line of immortalized human fibroblasts (Todaro et al., 1966). Isolated individual cells are small, polarized, and motile. Low-dose treatment with cytochalasin inhibits cytokinesis but permits nuclear and organelle multiplication. After drug washout, the resulting giants are typically discoid and very well spread (Lyass et al., 1984), showing active intracellular vesicle transport and characteristic leading-edge behavior symmetrically around the periphery.

Beads were coupled covalently to ConA or FN at saturating concentrations. The former is a lectin that binds sugar moieties present on many cell surface receptors, whereas the latter interacts specifically with integrins and induces adhesion-dependent signaling. When placed near the cell edge, the cell pulled beads of either type out of the optical trap after a period of ~1 min, or immediately after adhesion if the tweezers were extinguished. The beads then initiated a centripetal motion, which persisted for many minutes as the giant cells provide very long paths with an unambiguous frame of reference. An example is shown in Fig. 1 *a*.

Distinct radial regions in the membrane and cytoplasm

A time-lapse trace of bead position at equal time intervals in Fig. 1 *b* shows the clear separation of the cell into three distinct regions of motion: the lamella (I), an intermediate endoplasmic region (II), and the perinuclear (III). Note that the boundaries between regions are abrupt. In region I, beads display the canonical centripetal motion with an average velocity of ~1 μm/min. Within the same cell we see variability from 0.5 to 2 μm/min. The velocity of distant beads may differ, or that of a single bead may oscillate between these limits. At the boundary between regions I and II, beads undergo a sudden and significant increase in velocity. Beads placed at neighboring locations in region I experienced the increase in velocity at the same radius from the cell center, as shown, even if they pass the boundary at different times. They finally reach the perinuclear region (III) and continue to move randomly within a restricted space. Brownian motion typified by short, fast, random excursions was not observed in any region.

Centripetal motion in region I was indistinguishable for ConA- and FN-coated beads both in velocity and directionality, as seen in Fig. 1, *c–f*. A bead placed on the substrate immediately in front of the cell would be lifted by a lamellipodial extension and carried back to the lamella to initiate the centripetal movement. We note that, in the giant cells, the lamellipodia are not exaggerated in width, which remains ~5 μm. These were very active in extension and retraction to ruffles on the lamella. Together with the small width, this precluded a study of bead dynamics on the lamellipodium specifically. It was also clear that the bead motion was significantly slower than the retraction of lamellipodia into ruffles. Ruffles always overtook the beads. Notably, the instantaneous velocity of a bead was always maximum just when the cell drew it from the optical tweezers (not shown). This is in apparent agreement with previous observations of force accumulation, attributed on the lamellipodium to ligand-specific reinforcement (Choquet et al., 1997; Felsenfeld et al., 1999).

Region II was observed in most cells, but was variable in width so that its presence could be difficult to detect. Region III, in common with region I, appeared universally. There, the random wandering of the bead was analyzed as an anomalous diffusion, where the mean-squared displacement $\langle x^2(t)\rangle$ takes a scaling of $t^{3/2}$. Nocodazole treatment restores ordinary diffusion. These results have been reported separately (Caspi et al., 2000, 2001).

In contrast to the motion, adhesion of ConA and FN beads to the membrane was greatly dissimilar. Both types adhered near the cell edge, i.e., in region I. ConA beads adhered instantly there, whereas FN beads had to be held as long as 30 s in the optical tweezers before adhering. In regions II and III, FN beads failed entirely to adhere, whereas ConA beads adhered but remain stationary. They neither diffused nor moved directionally, nor could they be dragged laterally, drawn away leaving membrane tethers, nor removed with the optical tweezers. Thus, the membrane displays a clear stratification to two regions with respect to adhesion with the boundary at the junction of the lamella and endoplasm as revealed by the bead dynamics in Fig. 1. Although difficult to perceive a priori, this boundary also coincides with the presence of large vesicles excluded from region I. (Small transport vesicles and mitochondria appear throughout regions I and II.) The boundary is probably equivalent to a lamelloplasm/endoplasm boundary described previously, also on the basis of vesicle populations (Domnina et al., 1972).

Engulfment of centripetally moving beads

Giant cells were fixed immediately after optical observation and prepared for SEM. Previous knowledge of the beads' history in regions II and III is essential: they may have been placed there directly, or alternately have arrived by passage from region I. Using etched-grid coverslips it was possible to return to the same cell studied optically, and so to distinguish moving from stationary beads in the SEM. Beads which move in region I are engulfed into the cytoplasm. The initial stage of engulfment involves extension of a membrane fold surrounding the bead, as seen in Fig. 2 *a*. In Fig. 2, *b* and *c*, it is clearly seen that beads placed on the lamella are completely engulfed by the membrane while executing the centripetal motion.

Engulfment was observed for all beads, FN and ConA, that were placed on the lamella and initiated centripetal

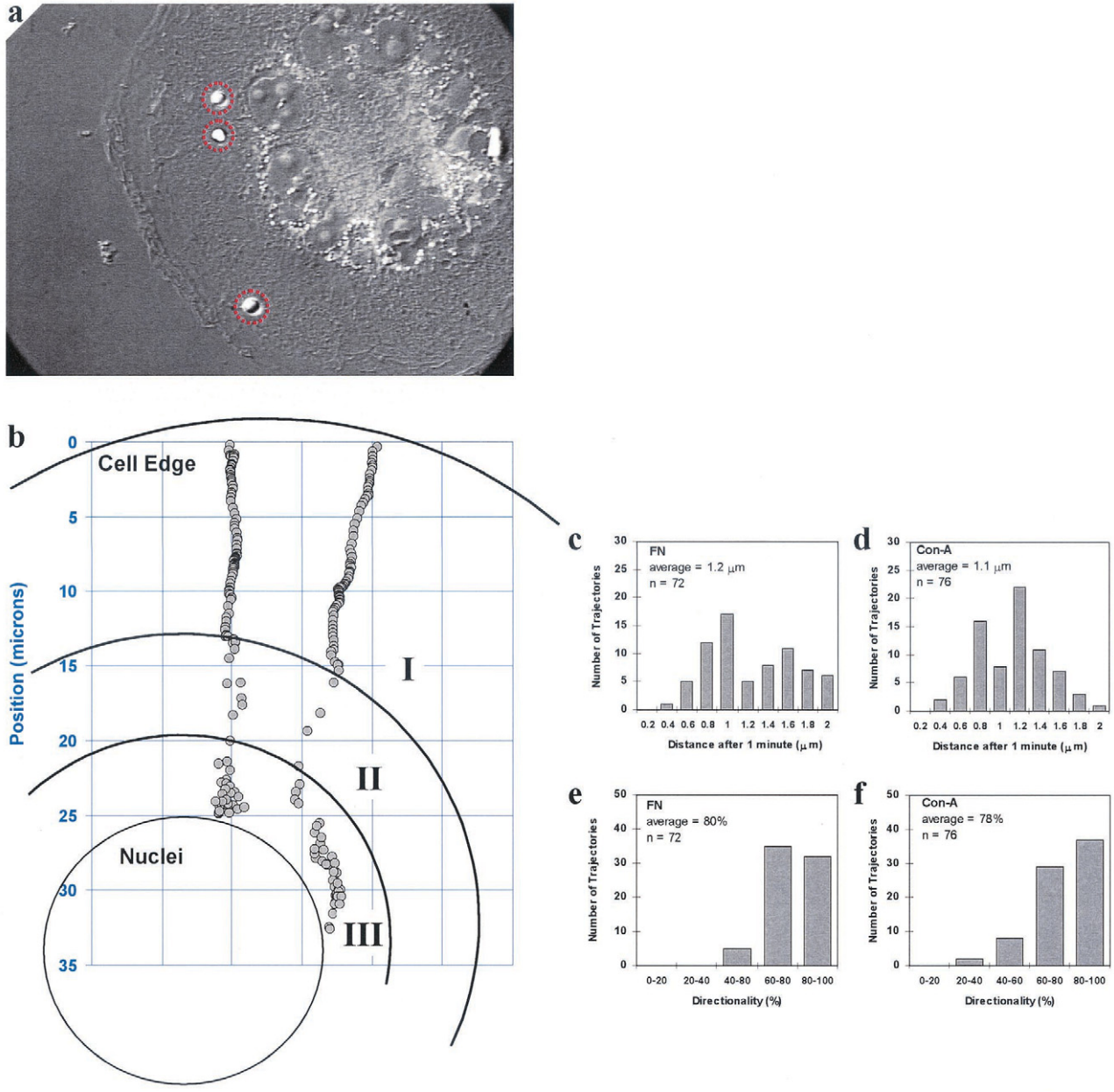

FIGURE 1 Bead movement on giant fibroblasts. (*a*) A typical multinuclear giant seen by DIC. The horizontal field of view is 120 μm. 3 μm beads are marked in red circles. (*b*) A time-lapse trace of two beads side-by-side displays three distinct regions of motion: slow and directed on the lamella (I), fast and directed in the endoplasm (II), and fast but nondirected near the nuclei (III). Points are shown at equal time intervals of 5 s; their separation indicates velocity. On the *right*, a compilation of directed velocity and directionality in region I shows no significant differences for beads coated by FN and ConA. (*c*) and (*d*) Histograms plot progress of beads along a straight path defined by their start- and endpoints at 60-s intervals. (*e*) and (*f*) Ratio of this directed progress divided by the actual path length executed by the bead, so that 100% indicates perfect directionality and 0% indicates motion perpendicular to the overall path. To match pervious definitions, the directionality ratio used here is identical to "distance fraction" (de Win et al., 1999) and is one over "persistency" (Euteneuer and Schliwa, 1984).

motion. The application of specific inhibitors notwithstanding (see below), not a single bead (of 40 beads on 12 samples) that was observed to move in the live studies was seen in the SEM resting on the membrane outside the cell, even if the fixation was performed immediately at the start of movement. Once the beads reached a zone of the cell significantly thicker than their diameter (regions II and III), they could no longer be observed in the SEM. They could be seen optically, however, throughout the stages of fixation and critical point drying. Thus the motion we observe in all three regions takes place within the cytoplasm and not on top of the cell membrane.

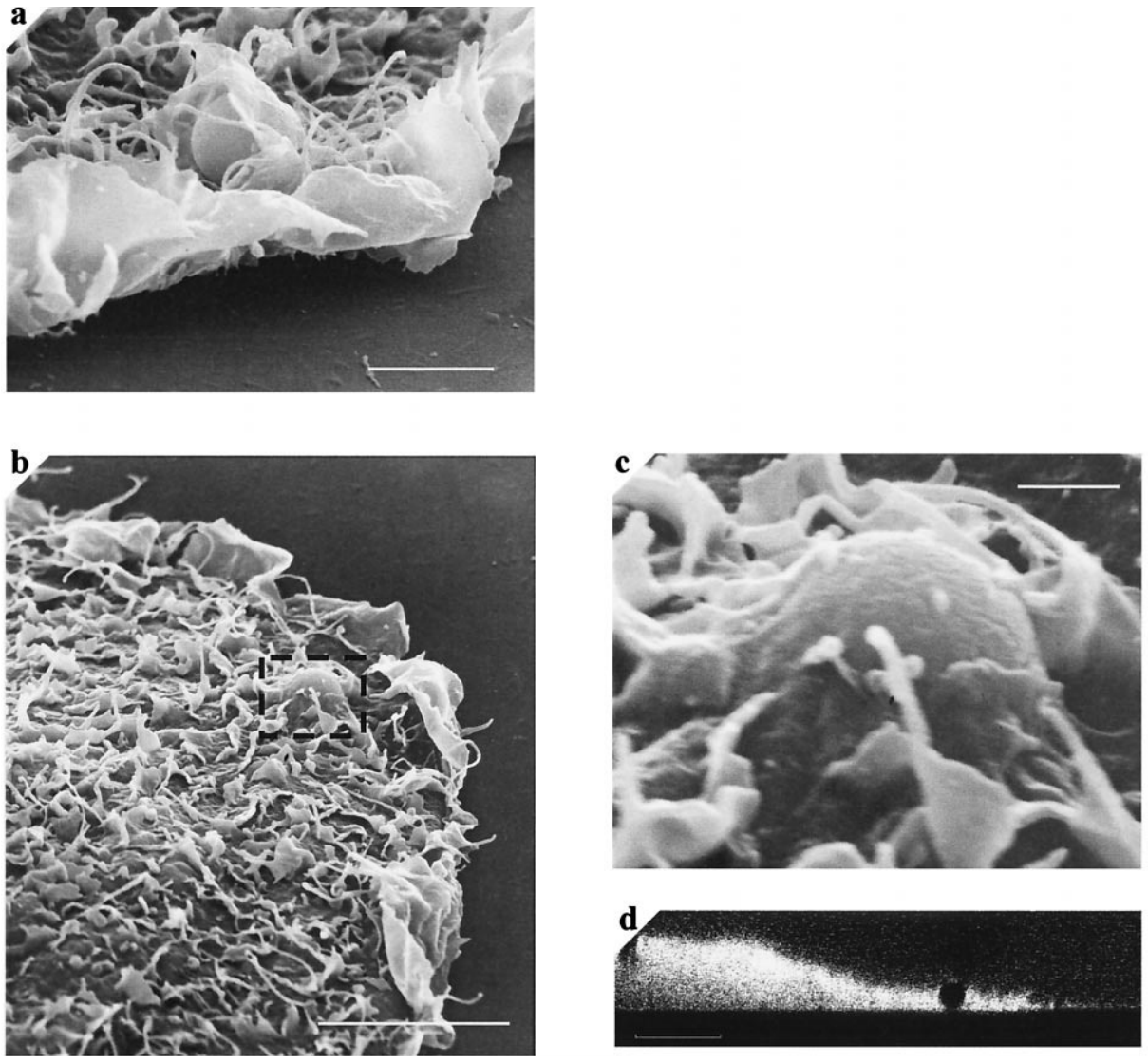

FIGURE 2 Moving beads in region I are engulfed into the cytoplasm. SEM and confocal microscopy follow optical observation and tracking of beads on the same cells. (*a*) The process of engulfment by which a membrane fold wraps over a bead. Scale bar = 3 μm. (*b*) A bead seen to move optically, marked by the *dashed box*, is clearly covered by plasma membrane. Scale bar = 10 μm. (*c*) An expanded view of the box shown in *b*. Scale bar = 1 μm. (*d*) A vertical section taken by confocal microscopy using rhodamine-phalloidin staining for actin. Note the spherical hole in the fluorescence indicating the bead. Scale bar = 10 μm. (SEM pictures were taken at high tilt, so scale measurements are distorted). Leaving the cells in serum-containing medium results in the strong membrane perturbances shown.

To investigate the structures of F-actin that may drive the bead, cells were stained with rhodamine-phalloidin and observed by standard epifluorescence and confocal microscopies. We did not observe any cables or other structures reminiscent of stress fibers leading to the bead, or alternately comet-tails behind the bead as have been found to drive *Listeria* motion (Tilney and Portnoy, 1989; Dabiri et al., 1990), or inductopodia as seen in neuronal growth cones (Thompson et al., 1996). Again, we observed in fluorescence the same beads that we had previously followed live and whose motion was blocked by fixation. We did notice a concentration of actin surrounding the bead, including a halo of fluorescence apparently above the bead (not shown). A vertical section by confocal microscopy, Fig. 2 *d*, shows the bead embedded in the lamella, confirming the engulfment in region I.

ConA beads placed on regions II and III adhered to the membrane without undergoing engulfment, as shown in Fig. 3 *a*. These beads were stationary. Moreover, when two beads were placed on the cell, one on region I and the other on region II, only the former moved. In some cases, upon reaching region II, the moving bead could be seen to pass underneath the stationary one without disturbing its position, as seen in Fig. 3 *b*. Thus, the bead which moves clearly does so entrained in the cytoplasm rather than on top of the dorsal surface.

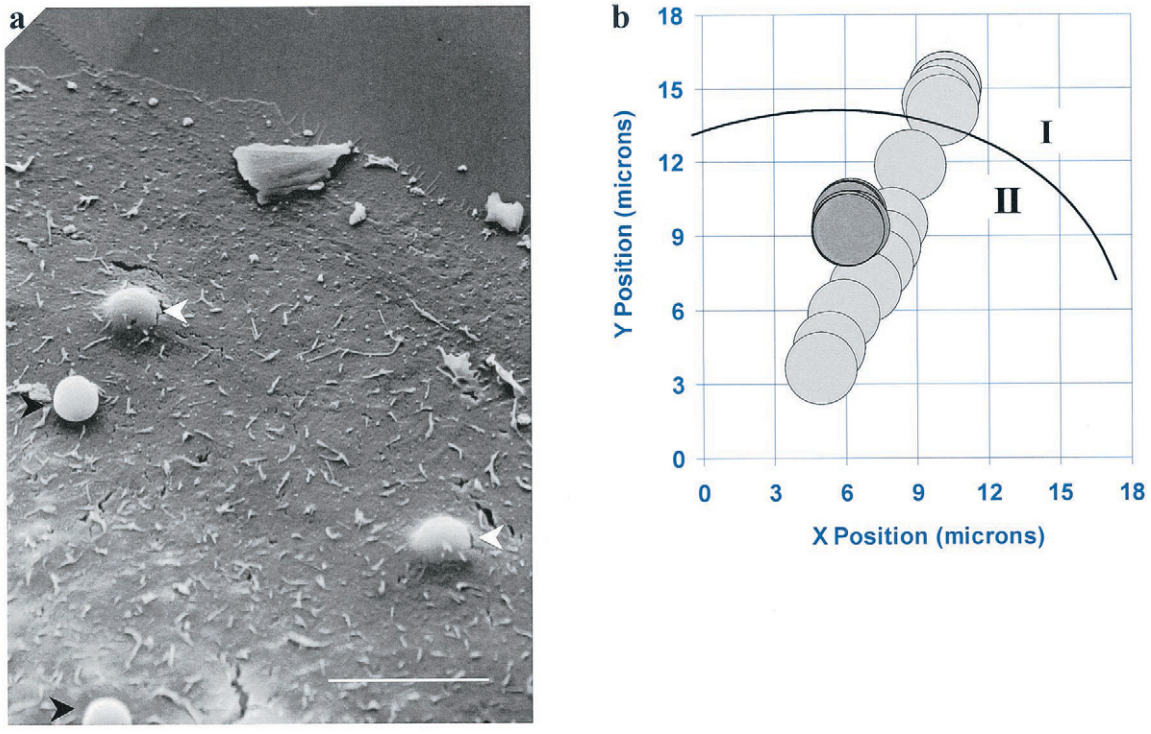

FIGURE 3 Engulfed beads move centripetally whereas membrane-bound beads are stationary. (*a*) Lamella-originated beads, seen to move optically in region I and marked by *white arrowheads*, are compared by SEM with beads placed directly on regions II and III, marked by *black arrowheads*. The former are engulfed and perform centripetal motion whereas the latter remain on top of the dorsal surface, and do not move. Scale bar = 10 μm. Serum-free medium causes a smoothing of the membrane, but does not interfere with engulfment or centripetal motion (Fig. 2). (*b*) An optical trace shows that a moving bead that entered from region I passes underneath a stationary one placed on region II. The time interval between points shown is 10 s and the symbol size represents the bead diameter.

Having observed that the bead motion takes place underneath the plane of the undisturbed dorsal surface, we developed a quantitative method to detect the bead height in live measurements. This permits instant observation and avoids any possibility that the engulfment may be a fixation artifact due to drying and shrinking of the cell. Using the optical tweezers, we could bring a second bead to the area in which we observe the motile one, and lower it onto the cell surface nearby. Only if both beads lie at the same height will they be in focus simultaneously. Quantitative measurements were made by brightfield illumination with parallel light (Strick et al., 1998). Diffraction rings appear surrounding the beads, Fig. 4 *a*, whose number and diameter provide a sensitive measure of the axial distance from the bead center to the plane of focus. The vertical distance between two beads can be measured accurately (Fig. 4 *b*) by comparing the images of the rings with a set of standard reference images, examples of which are shown in Fig. 4 *e*.

Using the method described above, we also measured the axial position of the bead during its motion, particularly at the initiation of the motion. Measurements of the motile bead height, compared with a stationary one fixed to the cover glass, show a motion downward (Fig. 4, *c* and *d*), i.e., toward the cover glass. In case the bead would move along the cell surface, we would expect an upward motion, as the slope of the cell surface rises from the edge toward the center. The downward motion along the centripetal path indicates a traction force that draws the bead into the cell.

Effect of cytoskeletal inhibitors on engulfment and centripetal movement

Several inhibitors of actomyosin contractile activity were applied in an attempt to distinguish molecular requirements for engulfment and centripetal motion. Results are displayed in the images of Fig. 5 for engulfment, and data of Table 1 for centripetal motion. We found that BDM and overexpression of caldesmon both inhibited engulfment entirely. BDM may have nonspecific effects including changes in the microtubule network (Krendel et al., 1998). Therefore we pursued the use of caldesmon to study the effect on centripetal motion on live cells. As a natural regulator of actomyosin interactions, it is likely to have a more specific action. We found that centripetal motion of the bead continues on region I even without engulfment,

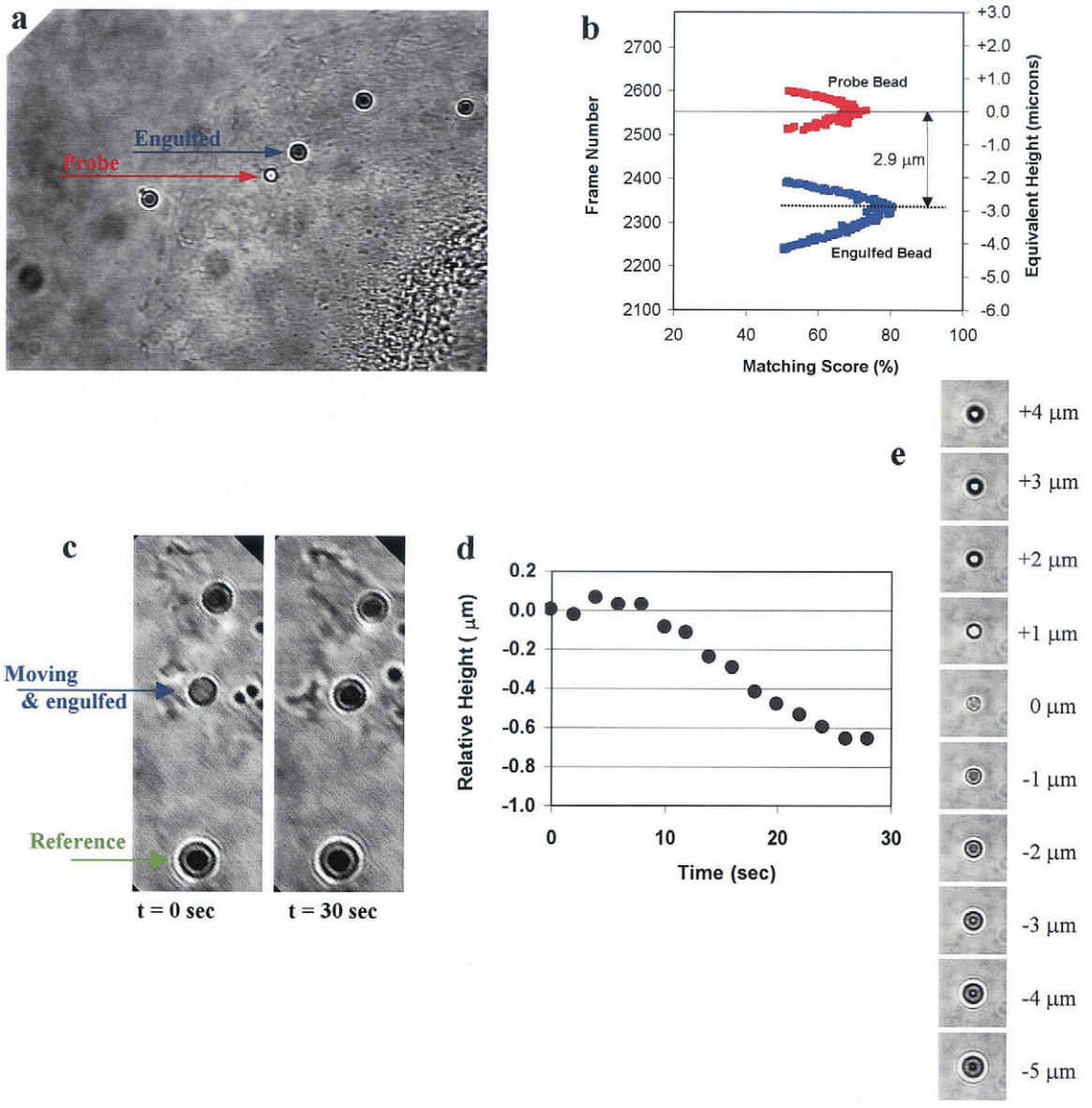

FIGURE 4 Vertical height measurements on live cells. (*a*) Diffraction rings surrounding beads reflect their heights with respect to the focal plane. Moving beads are compared with a probe bead held in the optical tweezers and brought to contact with the membrane. (*b*) A plot of frame number (*left axis*) or equivalent height (*right axis*) from the reference sequence versus the cross-correlation score between sample and reference images identifies a best-fit for each bead, and establishes the relative height between them. The panel on the right shows samples of reference images from a sequence showing the appearance of a bead at various heights from the focal plane. The actual reference sequence used for measurements had a height difference of 13 nm between successive frames. (*c*) Diffraction rings around a bead initiating centripetal motion compared with a stationary reference bead fixed to the cover glass at $t = 0$ and $t = 30$ s. (*d*) A plot of the height of the moving as function of time along the centripetal path. (*e*) A vertical scan across a bead fixed to the coverslip shows a sequence of images as a function of height with respect to the focal plane.

albeit at a velocity reduced to approximately one-third that observed on untreated cells. Nontransfected (i.e., nonfluorescent) cells in the same culture showed engulfment and centripetal bead movement similar to untreated cells. Caldesmon treatment was the only condition under which we observed centripetal motion without engulfment. H-7, a broad specificity kinase inhibitor effective in inhibiting overall cell contractility, inhibited neither engulfment nor centripetal motion. In addition, we depolymerized the microtubule network using nocodazole. This did not inhibit the engulfment, whereas the bead velocity in region I showed a significant increase.

DISCUSSION

The main results are summarized as follows: (1) moving beads were engulfed in multinuclear giant and normal SV80

TABLE 1 Influence of inhibitors on centripetal velocity

	Average velocity (μm/min)	Number of trajectories
Nontreated cells	1.13 ± 0.35	76
Caldesmon-transfected	0.33 ± 0.18	15
90 μM H-7	1.03 ± 0.27	12
10 μM Nocadazole	4.35 ± 1.55	6

Comparison of the average velocities of ConA coated beads on trajectories of 60-s duration. Depolymerizing the microtubule network caused a significant increase in the velocity. Direct inhibition of the actomyosin interaction by caldesmon transfection slowed the bead motion significantly. By contrast, H-7, which inhibits activity of myosin II via Rho kinase inhibition, did not induce any measurable change in the bead velocity.

cells; (2) bead motion persisted throughout the cytoplasm from the cell edge to the perinuclear region, but only when initiated on the lamella; (3) motion of engulfed beads was decoupled from that of stationary surface-adherent beads in the central regions; and (4) engulfment seems to be myosin-dependent.

Internal retrograde flow of actin provides a mechanism to explain the centripetal movement of beads engulfed into the lamella (region I). The inability of the optical tweezers to stop the particle motion indicates either collective motor protein activity or a directed flow of a solid or gel material, as the same optical trap could hold beads against a viscous liquid flow many times the observed velocities. The depolymerization of microtubules led to a significant increase in the rate of centripetal movement, pointing to actin or actomyosin activity as the driving agent. Retrograde flow of actin has been observed in peripheral lamella extending from epithelial cell clusters using a fluorescent speckle technique (Waterman-Storer et al., 1998). Beads engulfed in the lamella will be entrained in the internal retrograde flow, and their motion reflects its dynamics, rather than movement of membrane or membrane-bound structures throughout region I. In contrast to cell adhesion structures sensitive to specific ligand activation, the retrograde flow proceeds independently of the presence of entrained beads, and therefore, the qualitative insensitivity of the motion to bead coating is not surprising. Engulfment on the lamella was confirmed as well in nongiant SV80 cells. On reaching region III, lamella-originated bead movement loses directionality and exhibits a microtubule-dependent anomalous diffusion as reported previously (Caspi et al., 2000, 2001). We may speculate that the crossover from actin to microtubule dependence occurs in region II, as the instantaneous velocities observed there are more similar to those in region III than in region I.

To address the molecular requirements for engulfment and centripetal motion, we applied several inhibitors of actomyosin activity. All three block myosin-driven cell contractility but with different mechanisms of action. BDM is a small-molecule chemical inhibitor of actin-dependent myosin ATPase activity. It has been shown that BDM slows actin retrograde flow in neuronal growth cones in a concentration-dependent manner (Lin et al., 1996). Caldesmon is an endogenous regulator of the interaction between myosin heads and F-actin. We introduced it by transfection, using a GFP chimera to identify transfected and nontransfected cells in the same culture. Both BDM and caldesmon blocked engulfment entirely, and left the cell membrane uncharacteristically thin and flat. Both are expected to affect most or all myosin types to some extent, as they act at the level of the F-actin interaction with the myosin head. On caldesmon-treated cells, ConA beads continue to move along the surface of region I, albeit at a velocity approximately one-third that observed in untreated cells. We also used the kinase inhibitor H-7 to inhibit myosin II via dephosphorylation of the regulatory light chain. Among the targets of H-7 is Rho kinase (Uehata et al., 1997), whose inactivation releases the myosin light chain phosphatase from its inhibitory control, thereby leading to dephosphorylation of the myosin light chain and deactivation of myosin II. H-7 also acts directly to inhibit myosin light chain kinase. Treatment with H-7 did not block bead engulfment, nor did it affect the velocity of centripetal movement.

Overall cell contractility is, by contrast, affected in a phenomenologically similar way by BDM, caldesmon, and H-7. Inhibition of elastic substrate deformation and maturation of focal contacts was demonstrated using BDM (Balaban et al., 2001; Riveline et al. 2001) and caldesmon (Helfman et al., 1999). H-7 was also shown to inhibit substrate deformation (Tian et al., 1998), maturation of focal contacts (Helfman et al., 1999), and movement of cell matrix adhesion complexes (Zamir et al., 2000). The present results indicate that the force-generating mechanism driving centripetal movement of beads is distinct from that involved in cell contractility. The latter is closely associated with actin stress fibers anchored to the extracellular matrix via focal contacts and requires the activity of myosin II. The insensitivity of bead movement to H-7 indicates either that some other myosin is responsible for the motion of engulfed particles and by extension the actin retrograde flow, or alternately, that these processes do not require myosin activity at all. It remains possible that only some low level of myosin II activity is required for retrograde flow, which continues in the presence of H-7, or that this residual activity does not depend on phosphorylation of the regulatory light chain. The present results are in accord with the observation on sea urchin coelomocytes that treatment with the myosin light chain kinase inhibitor KT5926, specific in blocking myosin II activity, has a minimal effect on actin retrograde flow near the cell periphery (Henson et al., 1999). The effective block of engulfment by BDM and caldesmon, but not H-7, suggests involvement of an unconventional myosin. Myosin I, in particular, has been implicated in phagocytosis (Swanson et al., 1999).

In principle, centripetal movement of engulfed particles could depend on microtubule-associated motor proteins. To

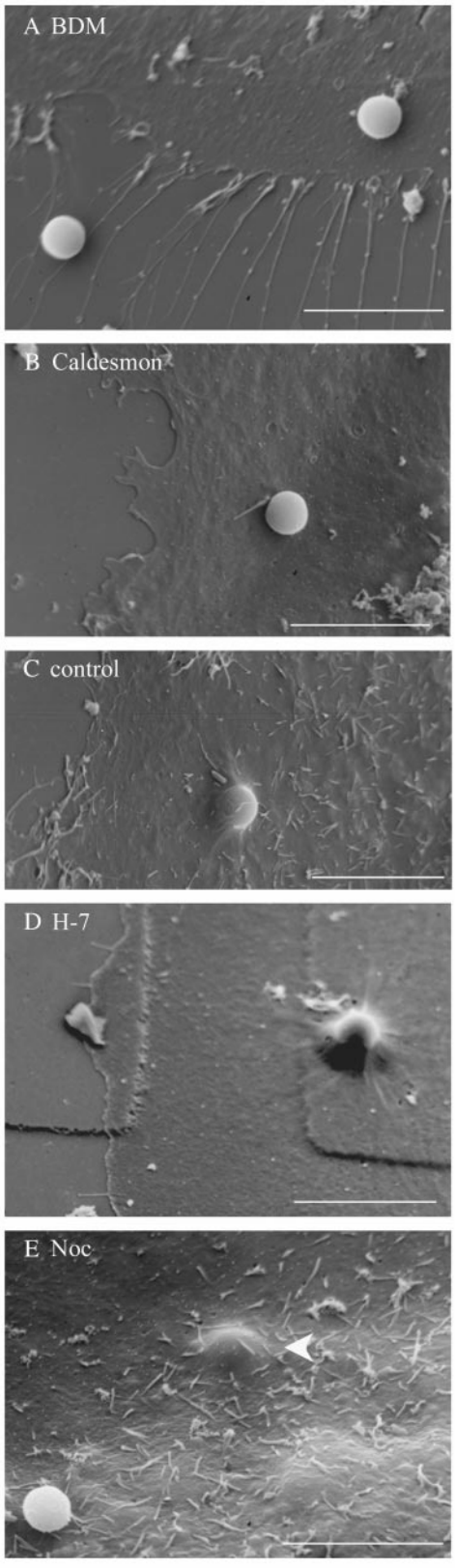

FIGURE 5 The influence of inhibitors on the engulfment. (*a*) BDM, a nonspecific inhibitor for the actin-myosin interaction, prevents engulfment. (*b*) In a cell transfected with caldesmon-GFP the bead was not engulfed. Centripetal motion was observed at significantly reduced velocity (see Table 1). (*c*) Beads are engulfed on region I in nontransfected (i.e., nonfluorescent) cells in the same sample as *b* above. (*d*) H-7, which inhibits activity of myosin II via inhibition of Rho kinase, did not prevent engulfment and did not stop the bead motion (see Table 1). (*e*) Engulfment is not inhibited by depolymerization of the microtubule network by nocodazole. The bead marked by the arrowhead was first placed on the cell periphery. It performed centripetal motion following engulfment. The bead at the lower left corner was placed initially at the center of the cell. It remained stationary and was not engulfed. Scale bars = 10 μm.

test this, we depolymerized the microtubule network using nocodazole. Engulfment was not affected. Instead of inhibiting centripetal bead movement, however, depolymerization of microtubules significantly enhanced the velocity. This might be because of a reduction of the effective viscosity of the cytosol or a result of biochemical recruitment of another cellular mechanism, perhaps even the activation of myosin II (Kolodney and Elson, 1995). An increase in the rate of actin flow attributable to microtubule depolymerization was also noted in *Xenopus laevis* oocytes (Benink et al., 2000).

Attachment of ConA beads to a submembranous cortex is observed in regions II and III, but this cortex is stationary. Beads are not engulfed in these regions. The fluid plasma membrane itself would be unable to resist shear forces implicit in dragging the beads with the optical tweezers, and we were unable to pull membrane tethers (Dai and Sheetz, 1995) although the beads clearly remained outside the cells. The lack of movement there implies the presence of a stationary, solid cortex (Svitkina et al., 1984), most likely of actin, bound to the beads via transmembrane receptors interacting with ConA. These observations indicate that the internal cytoskeletal networks are largely decoupled from the cortex supporting the membrane. The internal actin system in region I is dynamic whereas the actin supporting the membrane is stationary, at least in regions II and III. In region I, where engulfed particles move centripetally, we also observe decoupling of the bead from movement of surface features such as ruffles. Ruffles move significantly faster than the beads near the cell edge before they dissipate into the lamella. The bead movement, by contrast, is rather steady from the cell edge to the region I/II boundary. Distinct populations of actin, moving or stationary with respect to the cell motion, have been observed in locomoting fibroblasts (Cramer et al., 1997).

Although there is some ambiguity in nomenclature, retrograde flow is to be distinguished from "cortical actin flow" in that it takes place within the cytoplasmic volume rather than in membrane-associated actin sheet structures. Because evidence for proper cortical flow comes largely from observations of adherent particles (Sheetz et al., 1989), their attachment to the membrane or engulfment becomes a crucial factor. The question whether centripetal motion takes place above or below the free dorsal surface was addressed in the classic particle motility experiments (In-

gram, 1969; Abercrombie et al., 1970). A variety of tests was used, such as side view imaging, electron microscopy of sections of a cell known to be transporting, scraping away moving particles from living cells, and observation of particles falling off spontaneously after migration. It was also shown in a recent study that with extremely low ligand density of FN fragments, beads may move some distance and then detach at what seems to be the boundary between our regions I and II. The detachment clearly indicates that centripetal motion can occur without engulfment (Nishizaka et al., 2000). Nonetheless, the possibility of engulfment has largely been ignored, and it is difficult to draw conclusions in hindsight concerning other experiments that did not check specifically. Moreover, we note that the thin lamellipodium at the cell edge, on which many recent studies have focused, may behave quite differently from the more central regions on which we report. Several lines of evidence accumulated on living cells by fluorescence recovery after photobleaching (Lee et al., 1990), single particle tracking of individual receptors (de Brabander et al., 1991; Lee et al., 1991; Kusumi and Sako, 1996), and the latrunculin-sensitive immobilization of clathrin-coated pits (Gaidarov et al., 1999) may be interpreted as evidence against large-scale centripetal movements in the lamellar cortex.

Caldesmon transfection demonstrates that, under different conditions, movement of adherent beads may take place with or without engulfment even on the same cell type. The reduced velocity of bead movement could be explained by an effect of caldesmon (but not H-7) on an unconventional myosin driving retrograde flow, or by poor transmembrane coupling of the flow to the external particle.

CONCLUSION

A unifying picture can explain movement of engulfed and external particles. In both cases the driving force is provided by internal retrograde flow of actin throughout the lamella. The criterion for engulfment or external movement is based on membrane excess and the availability of specific myosins. When there is an excess of membrane, and the local membrane tension is accordingly low, surface-adherent beads are easily engulfed into the cytoplasm and are entrained in the flow directly. Nonengulfed particles still bind to the cell membrane by interaction with surface receptors. These couple through the membrane, directly or indirectly, to internal actin flow by intermittent binding and breaking of transmembrane connections, creating a sort of a slipping clutch. A similar mechanism may also operate in locomoting fibroblasts in which the external substrate couples to internal actin generating traction forces along the ventral surface (Munevar et al., 2001). We may suggest that centripetal movement of the engulfed bead is a localized consequence of the same tension generated between retrograde actin flow and the external substrate, where there is no opportunity for mechanical disengagement between the flow and the bead.

The authors have benefited from discussions with G. Borisy and B. Geiger. We are grateful to Elina Levina for conducting some preliminary experiments. This work was supported by grants from the Israel Science Foundation and the Minerva Research Foundation, La Fondation Raphael et Regina Levy, the Crown Foundation, and the Gerhard M. J. Schmidt Center for Supramolecular Architecture. A.D.B. is incumbent of the Joseph Moss chair in biomedical science. M.E. is an incumbent of the Delta career development chair.

REFERENCES

Abercrombie, M., J. E. Heaysman, and S. M. Pergum. 1970. The locomotion of fibroblasts in culture, III. movements of particles on the dorsal surface of the leading lamella. *Exp. Cell Res.* 62:389–392.

Anderson, K. I., Y. L. Wang, and J. V. Small. 1996. Coordination of protrusion and translocation of the keratocyte involves rolling of the cell body. *J. Cell Biol.* 134:1209–1218.

Ashkin, A., J. M. Dziedzic, J. E. Bjorkholm, and S. Chu. 1986. Observation of a single-beam gradient force optical trap for dielectric particles. *Opt. Lett.* 11:288–290.

Balaban, N. Q., U. S. Schwarz, D. Riveline, P. Goichberg, G. Tzur, I. Sabanay, D. Mahalu, S. Safran, A. Bershadsky, L. Addadi, and B. Geiger. 2001. Force and focal adhesion assembly: a close relationship studied using elastic micropatterned substrates. *Nat. Cell Biol.* 3:466–472.

Benink, H. A., C. A. Mandato, and W. M. Bement. 2000. Analysis of cortical flow models in vivo. *Mol. Biol. Cell.* 11:2553–2563.

Bershadsky, A., A. Chausovsky, E. Becker, A. Lyubimova, and B. Geiger. 1996. Involvement of microtubules in the control of adhesion-dependent signal transduction. *Curr. Biol.* 6:1279–1289.

Bretscher, M. S. 1984. Endocytosis: relation to capping and cell locomotion. *Science.* 224:681–686.

Caspi, A., R. Granek, and M. Elbaum. 2000. Enhanced diffusion in active intracellular transport. *Phys. Rev. Lett.* 85:5655–5658.

Caspi, A., R. Granek, and M. Elbaum. 2001. Anomalous diffusion in active intracellular transport. *Mater. Res. Soc. Symp. Proc.* 651:T1.2.

Choquet, D., D. P. Felsenfeld, and M. P. Sheetz. 1997. Extracellular matrix rigidity causes strengthening of integrin-cytoskeleton linkages. *Cell.* 88:39–48.

Cramer, L. P., M. Siebert, and T. J. Mitchison. 1997. Identification of novel graded polarity actin filament bundles in locomoting heart fibroblast: implications for the generation of motile force. *J. Cell Biol.* 136: 1287–1305.

Dabiri, G. A., J. M. Sanger, D. A. Portnoy, and F. S. Southwick. 1990. *Listeria monocytogenes* moves rapidly through the host-cell cytoplasm by inducing directional actin assembly. *Proc. Natl. Acad. Sci. U.S.A.* 87:6068–6072.

Dai, J., and M. P. Sheetz. 1995. Mechanical properties of neuronal growth cone membranes studied by tether formation with laser optical tweezers. *Biophys. J.* 68:988–996.

de Brabander, M., R. Nuydens, A. Ishihara, B. Holifield, K. Jacobson, and H. Geerts. 1991. Lateral diffusion and retrograde movements of individual cell surface components on single motile cells observed with nanovid microscopy. *J. Cell Biol.* 112:111–124.

de Win, A. H., E. S. Pierson, and J. Derksen. 1999. Rational analyses of organelle trajectories in tobacco pollen tubes reveal characteristics of the actomyosin cytoskeleton. *Biophys. J.* 76:1648–1658.

Domnina, L. V., O. Y. Ivanova, L. B. Margolis, L. V. Olshevskaja, Y. A. Rovensky, J. M. Vasiliev, and I. M. Gelfand. 1972. Defective formation of the lamellar cytoplasm by neoplastic fibroblasts. *Proc. Natl. Acad. Sci. U.S.A.* 69:248–252.

Euteneuer, U., and M. Schliwa. 1984. Persistent, directional motility of cells and cytoplasmic fragments in the absence of microtubules. *Nature.* 310:58–61.

Felsenfeld, D. P., P. L. Schwartzberg, A. Venegas, R. Tse, and M. P. Sheetz. 1999. Selective regulation of integrin-cytoskeleton interactions by the tyrosine kinase Src. *Nat. Cell Biol.* 1:200–206.

Gaidarov, I., F. Santini, R. A. Warren, and J. H. Keen. 1999. Spatial control of coated-pit dynamics in living cells. *Nat. Cell Biol.* 1:1–7.

Galbraith, C. G., and M. P. Sheetz. 1999. Keratocytes pull with similar forces on their dorsal and ventral surfaces. *J. Cell Biol.* 147:1313–1324.

Gelles, J., B. J. Schnapp, and M. P. Sheetz. 1988. Tracking kinesin-driven movements with nanometre-scale precision. *Nature.* 331:450–453.

Harris, A., and G. Dunn. 1972. Centripetal transport of attached particles on both surfaces of moving fibroblasts. *Exp. Cell Res.* 73:519–523.

Helfman, D. M., E. T. Levy, C. Berthier, M. Shtutman, D. Riveline, I. Grosheva, A. Lachish-Zalait, M. Elbaum, and A. D. Bershadsky. 1999. Caldesmon inhibits nonmuscle cell contractility and interferes with the formation of focal adhesions. *Mol. Biol. Cell.* 10:3097–3112.

Henson, J. H., T. M. Svitkina, A. R. Burns, H. E. Hughes, K. J. MacPartland, R. Nazarian, and G. G. Borisy. 1999. Two components of actin-based retrograde flow in sea urchin coelomocytes. *Mol. Biol. Cell.* 10:4075–4090.

Ingram, V. M. 1969. A side view of moving fibroblasts. *Nature.* 222: 641–644.

Jay, P. Y., and E. L. Elson. 1992. Surface particle transport mechanism independent of myosin II in *Dictyostelium*. *Nature.* 356:438–440.

Kolodney, M. S., and E. L. Elson. 1995. Contraction due to microtubule disruption is associated with increased phosphorylation of myosin regulatory light chain. *Proc. Natl. Acad. Sci. U.S.A.* 92:10252–10256.

Krendel, M., G. Sgourdas, and E. M. Bonder EM. 1998. Disassembly of actin filaments leads to increased rate and frequency of mitochondrial movement along microtubules. *Cell Motil. Cytoskeleton.* 40:368–378.

Kusumi, A., and Y. Sako. 1996. Cell surface organization by the membrane skeleton. *Curr. Opin. Cell Biol.* 8:566–574.

Lee, J., M. Gustafsson, K. E. Magnusson, and K. Jacobson. 1990. The direction of membrane lipid flow in locomoting polymorphonuclear leukocytes. *Science.* 247:1229–1233.

Lee, G. M., A. Ishihara, and K. A. Jacobson. 1991. Direct observation of Brownian motion of lipids in a membrane. *Proc. Natl. Acad. Sci. U.S.A.* 88:6274–6278.

Levenberg, S., B. Z. Katz, K. M. Yamada, and B. Geiger. 1998. Long-range and selective autoregulation of cell-cell or cell-matrix adhesions by cadherin or integrin ligands. *J. Cell Sci.* 111:347–357.

Lin, C. H., E. M. Espreafico, M. S. Mooseker, and P. Forscher. 1996. Myosin drives retrograde F-actin flow in neuronal growth cones. *Neuron.* 16:769–782.

Lin, C. H., and P. Forscher. 1995. Growth cone advance is inversely proportional to retrograde F-actin flow. *Neuron.* 14:763–771.

Lyass, L. A., A. D. Bershadsky, V. I. Gelfand, A. S. Serpinskaya, A. A. Stavrovskaya, J. M. Vasiliev, and I. M. Gelfand. 1984. Multinucleation-induced improvement of the spreading of transformed cells on the substratum. *Proc. Natl. Acad. Sci. U.S.A.* 81:3098–3102.

Munevar, S., Y. L. Wang, and M. Dembo. 2001. Traction force microscopy of migrating normal and H-*ras* transformed 3T3 fibroblasts. *Biophys. J.* 80:1744–1757.

Nishizaka, T., Q. Shi, and M. P. Sheetz. 2000. Position-dependent linkages of fibronectin-integrin-cytoskeleton. *Proc. Natl. Acad. Sci. U.S.A.* 97: 692–697.

Riveline, D., E. Zamir, N. Balaban, U. Schwarz, T. Ishizaki, S. Narumiya, Z. Kam, B. Geiger, and A. Bershadsky. 2001. Focal contacts as mechanosensors: externally applied local mechanical force induces growth of focal contacts by a mDia1-dependent and ROCK-independent mechanism. *J. Cell Biol.* 153:1175–1186.

Schmidt, C. E., A. F. Horwitz, D. A. Lauffenburger, and M. P. Sheetz. 1993. Integrin-cytoskeletal interactions in migrating fibroblasts are dynamic, asymmetric, and regulated. *J. Cell Biol.* 123:977–991.

Sheetz, M. P., S. Turney, H. Qian, and E. L. Elson. 1989. Nanometre-level analysis demonstrates that lipid flow does not drive membrane glycoprotein movements. *Nature.* 340:284–288.

Strick, T. R., J. F. Allemand, V. Croquette, and D. Bensimon. 1998. Physical approaches to study of DNA. *J. Stat. Phys.* 93:647–672.

Svitkina, T. M., A. A. Shevelev, A. D. Bershadsky, and V. I. Gelfand. 1984. Cytoskeleton of mouse embryo fibroblasts: electron microscopy of platinum replicas. *Eur. J. Cell Biol.* 34:64–74.

Swanson, J. A., M. T. Johnson, K. Beningo, P. Post, M. Mooseker, and N. Araki. 1999. A contractile activity that closes phagosomes in macrophages. *J. Cell Sci.* 112:307–316.

Theriot, J. A., and T. J. Mitchison. 1992. Comparison of actin and cell surface dynamics in motile fibroblasts. *J. Cell Biol.* 119:367–377.

Thompson, C., C. H. Lin, and P. Forscher. 1996. An *Aplysia* cell adhesion molecule associated with site-directed actin filament assembly in neuronal growth cones. *J. Cell Sci.* 109:2843–2854.

Tian, B., C. Millar, P. L. Kaufman, A. Bershadsky, E. Becker, and B. Geiger. 1998. Effects of H-7 on the iris and ciliary muscle in monkeys. *Arch. Ophthalmol.* 116:1070–1077.

Tilney, L. G., and D. A. Portnoy. 1989. Actin filaments and the growth, movement, and spread of the intracellular bacterial parasite, *Listeria monocytogenes*. *J. Cell Biol.* 109:1597–1608.

Todaro, G. J., H. Green, and M. R. Swift. 1966. Susceptibility of human diploid fibroblast strains to transformation by SV40 virus. *Science.* 153:1252–1254.

Uehata, M., T. Ishizaki, H. Satoh, T. Ono, T. Kawahara, T. Morishita, H. Tamakawa, K. Yamagami, J. Inui, M. Maekawa, and S. Narumiya. 1997. Calcium sensitization of smooth muscle mediated by a Rho-associated protein kinase in hypertension. *Nature.* 389:990–994.

Waterman-Storer, C. M., A. Desai, J. C. Bulinski, and E. D. Salmon. 1998. Fluorescent speckle microscopy, a method to visualize the dynamics of protein assemblies in living cells. *Curr. Biol.* 8:1227–1230.

Zamir, E., M. Katz, Y. Posen, N. Erez, K. M. Yamada, B. Z. Katz, S. Lin, D. C. Lin, A. D. Bershadsky, Z. Kam, and B. Geiger. 2000. Dynamics and segregation of cell-matrix adhesions in cultured fibroblasts. *Nat. Cell Biol.* 2:191–196.